SHEAR FAILURE OF A TRANSVERSELY POST-TENSIONED SKEWED BOX-BEAM BRIDGE

Andrzej S. Nowak, PhD, Dept. of Civil Engineering, University of Nebraska, Lincoln, NE
Carl Walker, PhD, PE, CW Consulting, LLC, Kalamazoo, MI
Vijay K. Saraf, PhD, PE, Exponent Failure Analysis Associates, Menlo Park, CA

ABSTRACT

The New Lothrop Road Bridge over Misteguay Creek in Shiawassee County, Michigan is a two-span, two-lane precast prestressed box-beam bridge with abutment and pier skews of 40 degrees. The 4ft. x 4ft. precast box beams span 132 ft (40 m), are grouted full depth between adjacent beams, and transversely post-tensioned. A 6.75 inch composite concrete slab was placed over the box beams. The bridge was designed for an HS-20 loading according to AASHTO design standards and was constructed in an agricultural area where trucks heavily loaded with sugar beets were common. After the bridge was put into service, large shear cracks developed in the exterior webs of the exterior beams adjacent to the obtuse angle corners of the skewed ends over both the abutments and the center pier. The design was reviewed using AASHTO design methods and showed no problem with the beam web shear design. The design and subsequent analysis both used the standard method of distributing a percentage of the truck lane loading to the individual beams. A finite element computer analysis was performed and the computer runs showed that the laterally post-tensioned bridge actually performed as a large flat plate rather than as individual beams. The flat plate carried the loads diagonally across the bridge in the stiffest direction between the obtuse corners of the plates. When shear stresses were calculated for the exterior webs of the box beams using the forces from the FEA, they were greatly in excess of allowable AASHTO stresses. As remediation, vertical shear post-tensioning was installed adjacent to the over-stressed webs and the bridge was put back in service.

Keywords: Prestressed box-beams, shear cracks, skew, finite element method.

INTRODUCTION

The objective of the paper is to present the results of structural analysis carried out for verification of the load carrying capacity of the New Lothrop Bridge located in Michigan. It consists of two identical spans, each with a center-to-center bearing span length of 132 ft (40m). The subject bridge showed signs of distress shortly after the completion of construction. These signs of distress included diagonal cracks (or shear cracks) near the obtuse corners of both spans, a minor tensile crack (or bending crack) close to mid-span of one span, and residual deflection in both spans. The presence of one minute tensile crack in one girder in only one span does not indicate a structural pattern and is most likely due to a local phenomenon relating to the material quality or the construction process. However, the presence of the shear cracks on exterior webs in both spans and the residual deflection in both spans indicate a condition related to the structural behavior of the entire structure.

Each span consists of nine 48 inch x 48 inch (1,200mm x 1,200mm) prestressed concrete box-beams, which are transversely post-tensioned. The cross section of a fascia beam is shown in Fig. 1. Each box beam has 42 strands. Original design of the bridge superstructure was based on tables provided in Michigan Bridge Design Guide circa 1992. Table 1, reproduced from the Michigan Bridge Design Guide, shows the maximum allowable span lengths for 48-inch (1,200 mm) prestressed box beams. According to the table the maximum allowable span length for the chosen combinations of box beams (nine 48-inch box beams, 2 lanes) and number of strands (42 each with an area of 0.153 $in.^2$ or 98.7 mm^2) is 132.0 ft (40m). Which indicates that the designed structure satisfies MDOT guidelines and is not expected to have any distress under maximum allowable Michigan loads.

Table 1. MDOT Table for Maximum Span Lengths (in ft) for 48" Prestressed Box Beams

Strands	6 beams 2 Lanes	7 beams 2 Lanes	8 beams 2 Lanes	9 beams 2 Lanes	10 beams 3 Lanes	11 beams 3 Lanes
36	116	119	121	123	120	122
38	118	122	124	126	124	125
40	122	125	127	129	126	128
42	124	128	130	**132**	129	131
44	127	129	131	-	130	-

Note 1 ft = 0.305m

The purpose of this analysis is to check if the bridge design satisfies the requirements specified by AASHTO Specifications applicable at the time of design and construction.

VERIFICATION OF THE DESIGN ACCORDING TO AASHTO

A comprehensive design check was performed for the New Lothrop Bridge in 1996. Both serviceability stresses and ultimate limit states were checked according to the AASHTO

Standard Specifications for Bridge Design (1992) and AASHTO Guide Specifications for Distribution of Loads for Highway Bridges (1994). Calculations were performed for the following two cases:

a) Design Check
For design check, following loads were considered: self weight of the girder, concrete in gaps, 6 inch (150mm) thick concrete slab, 25 psf (1.2kPa) future wearing surface, parapet and railings, and HS20 live load. Design compressive strength of concrete was 7,000 psi.

b) Check of Existing Structure
For these calculations, following loads were considered: self weight of the girder, concrete in gaps, 6.75 inch (170mm) thick actual concrete slab, no future wearing surface, parapet and railings, and no live load.

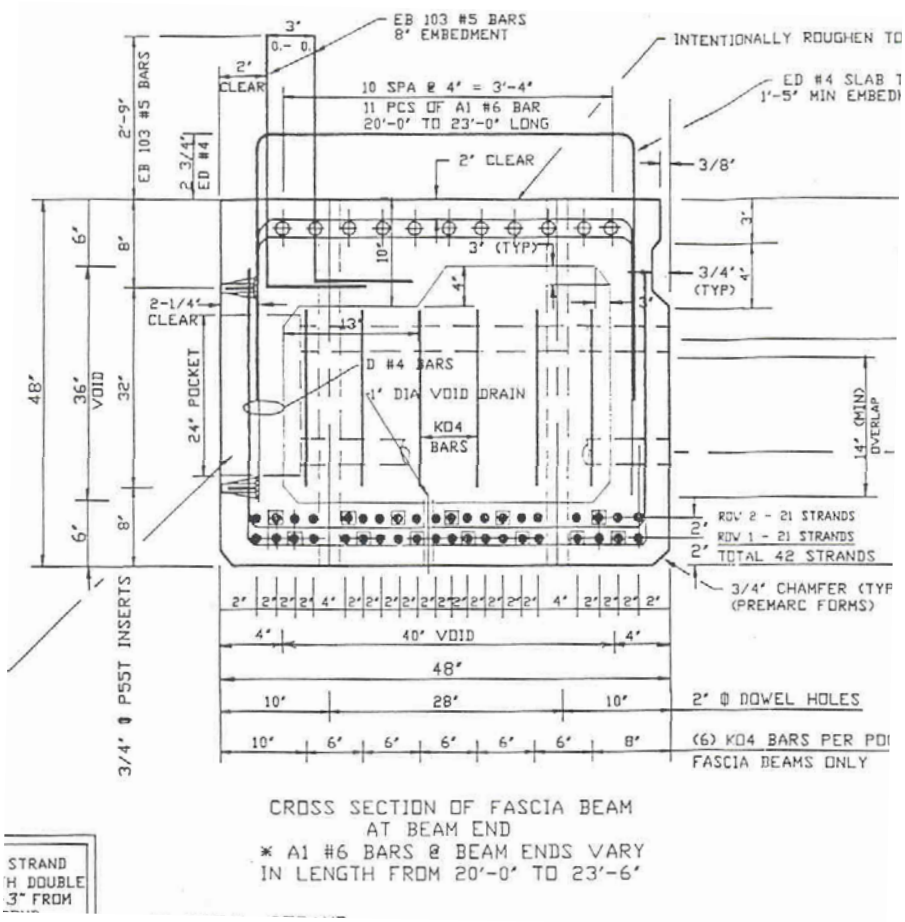

Fig. 1. Cross Section of a Fascia Box Beam at Beam End.

The results of a traditional AASHTO analysis are shown in Table 2 for exterior (fascia) beam, and Table 3 for interior (next to fascia) beam. For exterior and interior girders, the ultimate bending moments at mid-span are slightly higher than the limit specified by AASHTO (1992). The ultimate shear at 6 ft (1.8m) from the center-line of supports is within the AASHTO specified limits. Two serviceability limit states (tension at bottom of composite section and compression at top of girder in the composite section) exceed the allowable limits.

An extensive study of load distribution factors was performed as NCHRP project and resulted in AASHTO Guide Specifications for Distribution of Loads for Highway Bridges (1994). The girder distribution factors and correction factors for skew supports originally introduced in this AASHTO Guide (1994) are very similar to those retained in current AASHTO Specifications (2004). It confirms that the load distribution factors from AASHTO (1992) are often inaccurate. In particular, they do not account for the effect of skew of the bridge on the live load distribution.

Therefore, the calculations were also carried out using load distribution factors specified by AASHTO Guide (1994), as shown in right hand column of Tables 2 and 3. All ultimate limit states are satisfied. Two serviceability limit states (tension at bottom of composite section and compression at top of girder in the composite section) exceed the allowable limits. However, the live load distribution factors used in calculations may not be accurate for spans larger than 120 ft (36m). In such cases, AASHTO Guide (1994) suggests additional analysis of the structure. Therefore, the results were further updated using finite element analysis, which is presented in the following parts of the paper.

The results of the check for the existing structure (with no future wearing surface and no live load), using traditional AASHTO analysis, are shown in Table 4. Results indicate that the compressive stress at top of the interior girder slightly exceeds the allowable limit. The tensile stress at the mid-span and the ultimate moment and shear values are within the AASHTO allowable limits.

Table 2. Summary of Design Check for Exterior Girder Using AASHTO Specifications

Limit States	Allowable Stress / Factored Capacity	Stress at Service / Factored Loads	
Composite Section	AASHTO (1992)	AASHTO (1992)	Guide Spec.(1994)
Stress at top of girder	2,800 psi	3,170 psi	3,060 psi
Stress at bottom of girder	-500 psi	-1,200 psi	-1,020 psi
Stress at top of slab	1,800 psi	780 psi	630 psi
Ultimate moment	6,500 k-ft	6,740 k-ft	6,245 k-ft
Ultimate Shear	234 k	190 k	220 k

Table 3. Summary of Design Check for Interior Girder Using AASHTO Specifications

Limit States	Allowable Stress / Factored Capacity	Stress at Service / Factored Loads	
Composite Section	AASHTO (1992)	AASHTO (1992)	Guide Spec.(1994)
Stress at top of girder	2,800 psi	3,350 psi	3,230 psi
Stress at bottom of girder	-500 psi	-1,115 psi	-935 psi
Stress at top of slab	1,800 psi	805 psi	650 psi
Ultimate moment	6,500 k-ft	6,580 k-ft	6,080 k-ft
Ultimate Shear	234 k	186 k	215 k

Table 4. Summary of Results for Existing Structure Using AASHTO Specifications

Limit States	Allowable Stress / Factored Capacity	Stress at Service / Factored Loads	
Composite Section	AASHTO (1992)	AASHTO (1992)	Guide Spec.(1994)
Stress at top of girder	2,800 psi	2,720 psi	2,880 psi
Stress at bottom of girder	-500 psi	-475 psi	-375 psi
Stress at top of slab	1,800 psi	86 psi	88 psi
Ultimate moment	6,600 k-ft	4,750 k-ft	4,570 k-ft
Ultimate Shear	234 k	130 k	127 k

FINITE ELEMENT ANALYSIS

The live load distribution factor suggested by AASHTO guide specification (1994) is not applicable for spans longer than 120 ft (36m). For this study it was decided to use finite element analysis (FEA) to determine more accurate live load distribution factor. However, the change in the live load distribution factor as compared to the value suggested by AASHTO guide specification is expected to be very small. Therefore, the refined design check using FEA for live load distribution factor alone would likely yield the same conclusions derived earlier based on traditional analysis. However, the conclusions based on traditional AASHTO analysis are completely different than what the cracking indicates in the existing structure. Therefore, in addition to the live load distribution for HS20 load, it was decided to also investigate the dead load distribution for the weight of composite slab and 25 psf (1.2kPa) future wearing surface using the finite element modeling.

Before the transverse post-tensioning, the girders act individually and are not affected by the skew. However, after the transverse post-tensioning, they start acting as a slab and the distribution of additional dead load, i.e. slab, future wearing surface, parapets and railings, is considerably different than that in a straight bridge. Two finite element models of the bridge were prepared using the computer program ABAQUS (1998). A three-dimensional 4-node shell element S4R, that allows transverse shear deformations, was used in both models.

Slab Model

In this model, the structure was modeled as a continuous slab using plate elements with pin and roller supports at ends (i.e. the effect of elastomeric bearings is not considered). The finite element mesh for the model is shown in Fig. 2. The uniform support provided at abutment and pier was modeled as 19 equally spaced supports. The FEA showed that for both the uniformly distributed dead load and HS20 live load the mid-span moments were smaller than that in a straight bridge. Also, a very high concentration of shear stresses was observed in the edge close to the obtuse corner of the structure. As shown in Fig. 3 the extent of this concentration is limited to within the 2 ft (0.6m) of the edge (or the exterior girder) only. This indicates that the shear force due to the distributed dead load applied after the transverse post-tensioning should be amplified to account for this stress concentration. It is also noted, that the area of this shear concentration coincides with the location of the existing shear (or diagonal) cracks on the fascia beams. Several slab models with varying degree of skew were prepared to study the effect of skew on the concentration of shear or support reactions at the obtuse corner. Fig. 4 shows the support reactions with skew angles from 0 to 50 degrees. For 50 degree skew angle, the support reaction in the first support from the obtuse corner increases up to 10.4 times that for no skew. However, the increase in maximum shear stress is only about 6 times that of a slab with no skew.

The slab model is useful in showing the presence of the shear stress concentration at the obtuse corners. However, in the actual structure, most of the shear is carried by the girder webs, which are spaced at 4 ft (1.2m) from each other. Although the overall shear

distribution pattern in slab and the actual structure would be very similar, the actual values of shear stress/force might differ. Therefore, a more refined model consisting of webs and flanges (i.e. adjacent boxes) was prepared for further investigation.

Fig. 2. Finite Element Mesh for Slab Model.

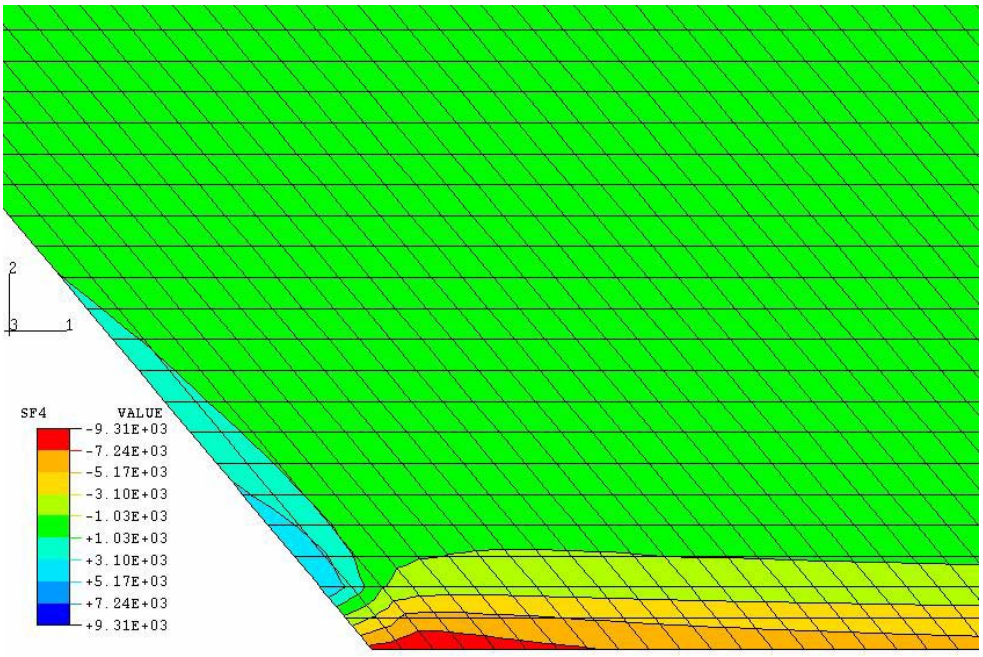

Fig. 3. Shear Stress Concentration in Obtuse Corner - Slab Model.

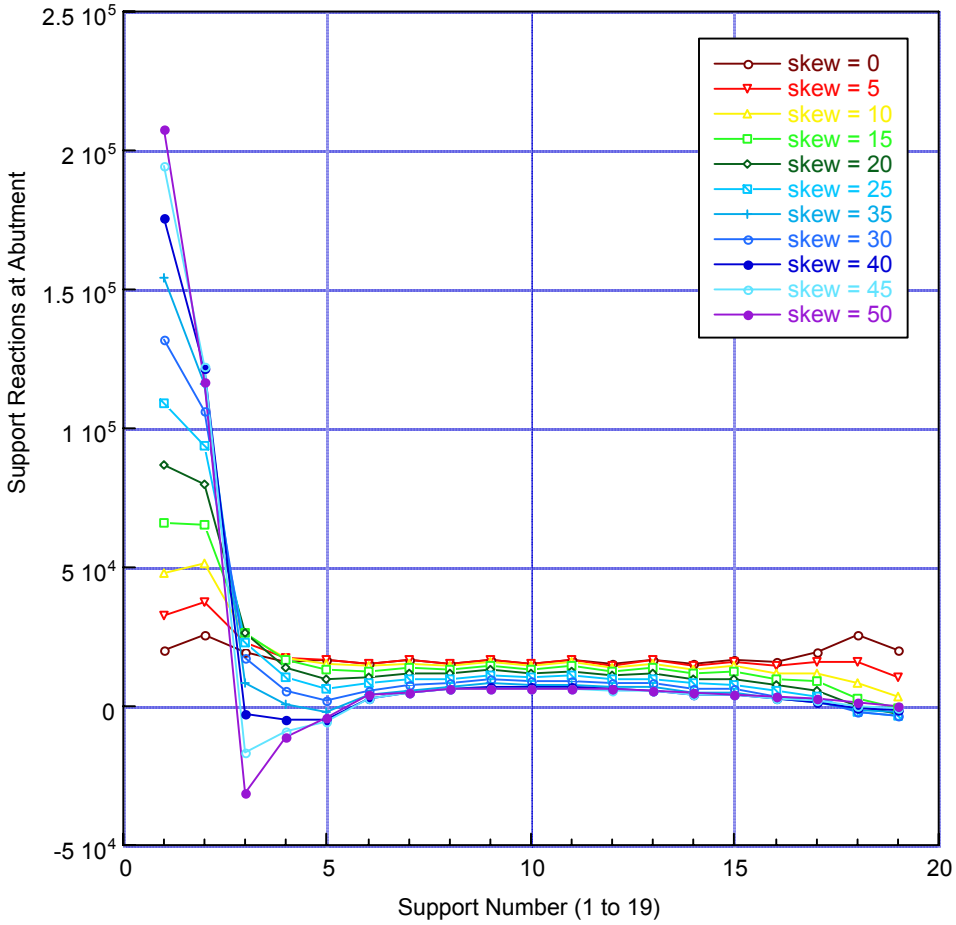

Fig. 4. Support Reaction verses Skew Angle - Slab Model.

Box Model

In this model, the bridge was treated as a combination of boxes. For each box, webs and flanges were modeled as three-dimensional shell elements (allowing shear deformations). The interior webs of adjacent girders were assumed to act together i.e. they were modeled using a single layer of shell elements, each with double the thickness of an interior web. First the supports were modeled as pins and rollers and the end blocks and diaphragms were ignored. Fig. 5 and Fig. 6 show the plan and cross-sectional view of the box model. However, as shown in Fig. 7, the support reactions obtained from the model lack the continuity in transverse direction. Therefore, two other models were prepared by sequentially adding, to the first model, the end blocks and diaphragms within each box and the

elastomeric bearings under each support. As shown in Figs. 7 and 8, this resulted in significant improvement in transverse distribution of support reactions and shear force. The results from the box model with end blocks and diaphragms and elastomeric bearings as springs were used to revise the calculations by traditional AASHTO analysis. The shear stress concentration at the obtuse corner obtained from this model is shown in Fig. 9. The distribution of shear stress in the exterior web is shown in Fig. 10.

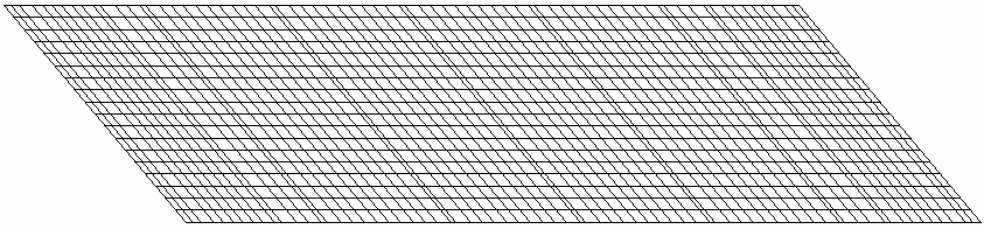

Fig. 5. Plan View of the Finite Element Mesh for Box Model.

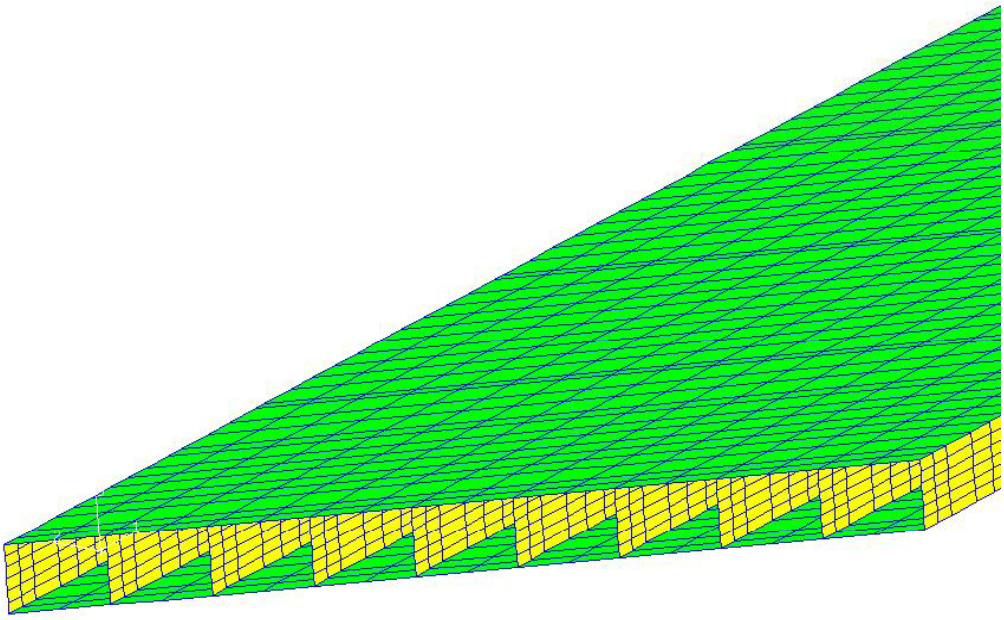

Fig. 6. Cross-Sectional View of the Finite Element Mesh for Box Model.

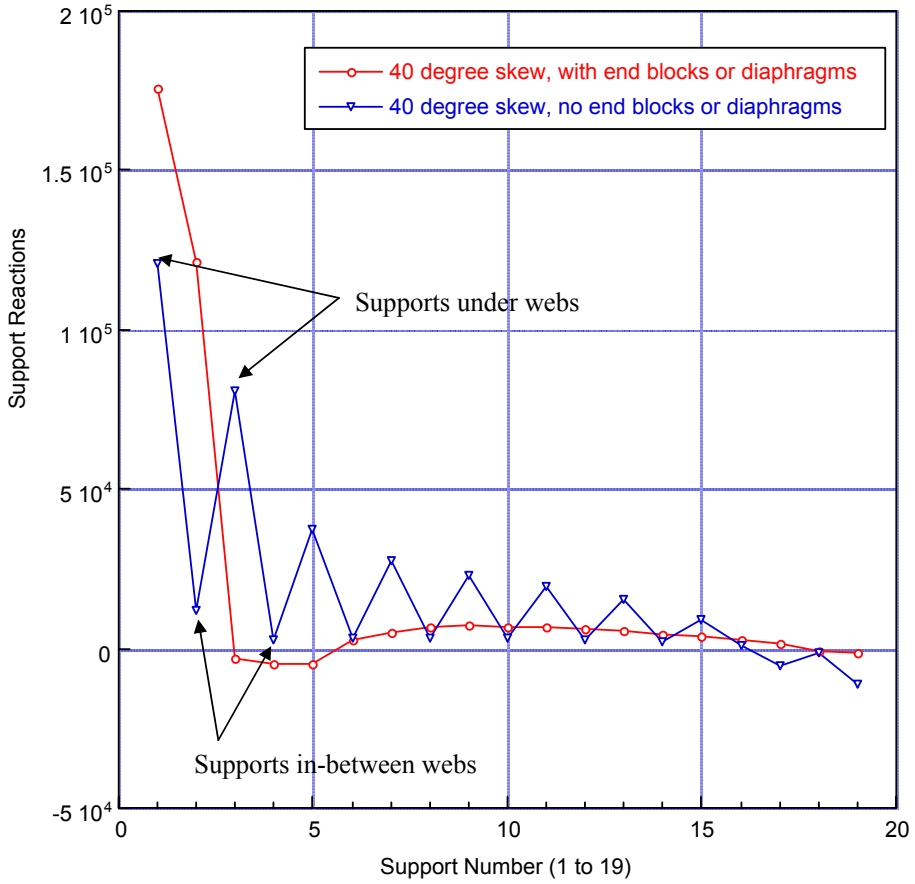

Fig. 7. Effect of End Blocks and Diaphragms on Support Reaction - Box Model.

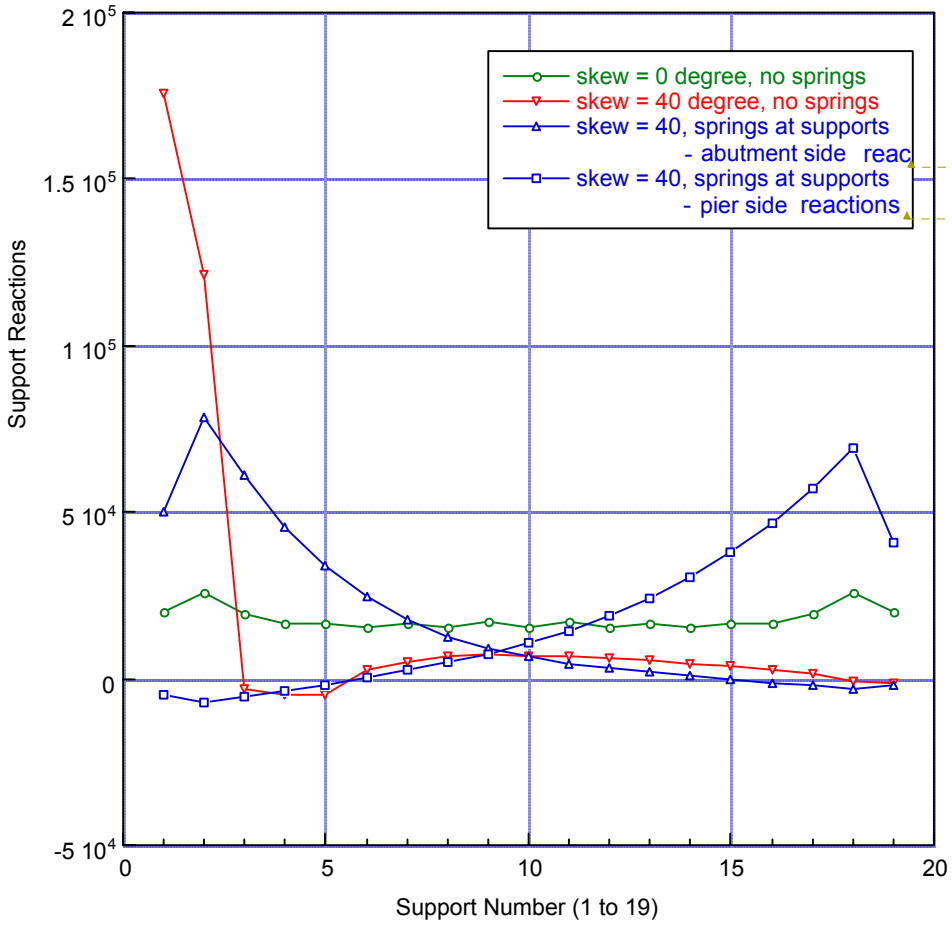

Formatted: Font: (Default) Arial, 11 pt, Font color: Blue

Formatted: Font: (Default) Arial, 11 pt, Font color: Blue

Fig. 8. Effect of Bearings on Support Reactions - Box Model.

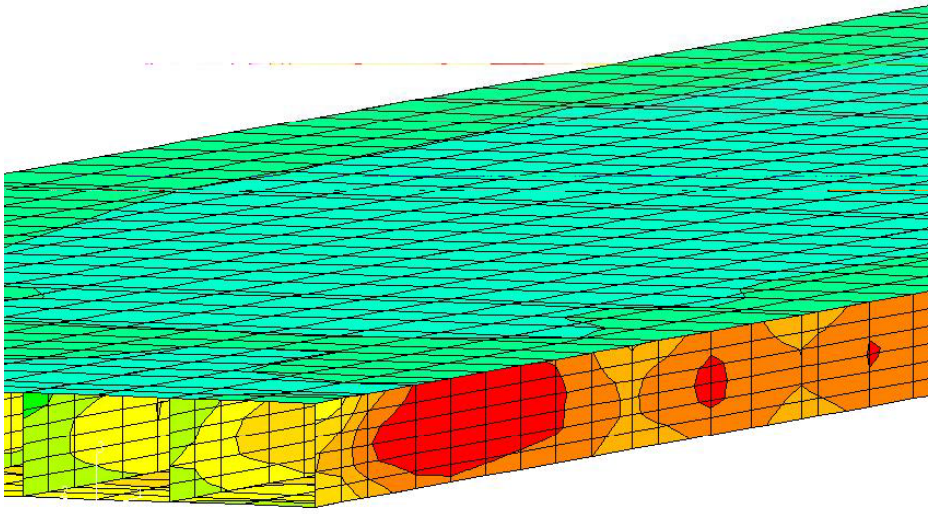

Fig. 9. Shear Stress Concentration at the Obtuse Corner - Box Model.

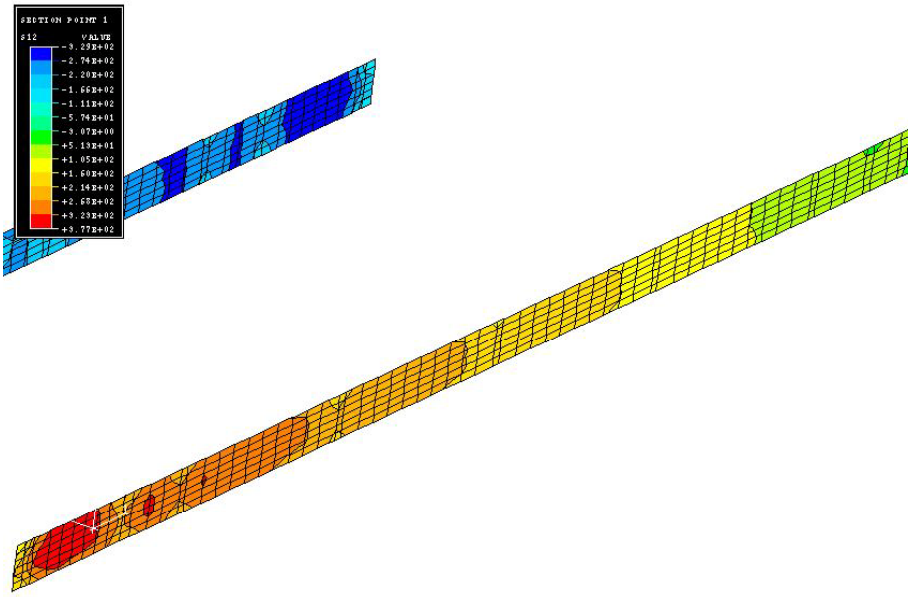

Fig. 10. Shear Stress Distribution along the Exterior Web - Box Model.

Summary of Finite Element Results - Box Model

The area of high shear concentration, shown in Fig. 9 and Fig. 10, coincides with the existing shear cracks in exterior girders. The results also suggest that other girders carry much smaller shear. The actual load distribution on this bridge is significantly different than that interpreted by AASHTO (1992) and AASHTO guide specification (1994) provisions. In particular, the mid-span moments due to superimposed dead load and HS20 live load were much smaller than those based on AASHTO Specifications. And the maximum shear forces due to distributed superimposed dead loads were significantly larger than those predicted by AASHTO Specifications.

As shown in Table 5, the exterior girder of the bridge, as designed, satisfies all AASHTO requirements except the serviceability requirement for tensile stress at the bottom of the girder close to mid-span, and the ultimate shear capacity close to supports. For interior girder of the bridge, the compressive stress at top of the girder, and the tensile stress at bottom of the girder slightly exceed the AASHTO specified limits.

Table 6 shows the results of the analysis performed for the existing structure, i.e. with 6.75 inch (170mm) slab, no future wearing surface, and no live load. All serviceability and ultimate limit states are satisfied. The ultimate (factored) shear in exterior web of the fascia beam is considerably higher than that computed using traditional AASHTO analysis (Table 4), and is slightly lower than the AASHTO allowable shear. The findings of the finite element study are much more consistent with the field observations than those predicted by traditional AASHTO analysis.

As remediation, vertical shear post-tensioning was installed adjacent to the over-stressed webs and the bridge was put back in service.

Table 5. Summary of Design Check for Exterior and Interior Girders Using Box Girder FEA

Limit States		Allowable Stress / Factored Capacity	Stress at Service / Factored Loads	
Composite Section		AASHTO (1992)	Exterior Girder	Interior Girder
Stress at top of girder		2,800 psi	2,750 psi	2,890 psi
Stress at bottom of girder		-500 psi	-640 psi	-530 psi
Stress at top of slab		1,800 psi	470 psi	480 psi
Ultimate moment		6,500 k-ft	5,530 k-ft	5,360 k-ft
Ultimate Shear	Ext. web only	117 k	189 k	112 k
	Int. web only	117 k	112 k	-
	Total per girder	234 k	301 k	224 k

Table 6. Summary of Results for Existing Structure Using Box Girder FEA

Limit States		Allowable Stress / Factored Capacity	Stress at Service / Factored Loads	
Composite Section		AASHTO (1992)	Exterior Girder	Interior Girder
Stress at top of girder		2,800 psi	2,500 psi	2,630 psi
Stress at bottom of girder		-500 psi	-215 psi	-100 psi
Stress at top of slab		1,800 psi	64 psi	66 psi
Ultimate moment		6,600 k-ft	4,420 k-ft	4,240 k-ft
Ultimate Shear	Ext. web only	117 k	114 k	77 k
	Int. web only	117 k	77 k	-
	Total per girder	234 k	191 k	154 k

CONCLUSIONS

The observed shear cracking in a box beam bridge with a considerable skew required an investigation of the causes. The analysis was performed using the traditional approach following AASHTO Specifications (1992) and by advanced finite element method (ABAQUS). The design reviewed using AASHTO design methods showed no problem with the beam web shear design. The design and subsequent analysis both used the standard method of distributing a percentage of the truck lane loading to the individual beams. The

finite element computer analysis showed that the laterally post-tensioned bridge actually performed as a large flat plate rather than as individual beams. The flat plate carried the loads diagonally across the bridge in the stiffest direction between the obtuse corners of the plates. When shear strength was calculated for the exterior webs of the box beams using the forces from the FEA, it was greatly in excess of allowable AASHTO shear capacity.

ACKNOWLEDGEMENTS

The authors acknowledge the assistance of current and former research staff and graduate students at the University of Michigan.

REFERENCES

1) AASHTO, Standard Specifications for Highway Bridges, 15th Edition, Washington, D.C., 19922
2) AASHTO, Guide Specifications for Distribution of Loads for Highway Bridges, Washington., D.C., 1994
3) ABAQUS Manual v. 5.8, Hibbitt, Karlsson & Sorensen, Inc., Pawtucket, RI, (1998).